COMMUNICATIONS PHYSICS

ARTICLE

https://doi.org/10.1038/s42005-019-0260-3 OPEN

Relaxion stars and their detection via atomic physics

Abhishek Banerjee[1], Dmitry Budker[2,3], Joshua Eby[1*], Hyungjin Kim[1] & Gilad Perez[1]

The cosmological relaxion can address the hierarchy problem, while its coherent oscillations can constitute dark matter in the present universe. We consider the possibility that the relaxion forms gravitationally bound objects that we denote as relaxion stars. The density of these stars would be higher than that of the local dark matter density, resulting in enhanced signals in table-top detectors, among others. Furthermore, we raise the possibility that these objects may be trapped by an external gravitational potential, such as that of the Earth or the Sun. This leads to formation of relaxion halos of even greater density. We discuss several interesting implications of relaxion halos, as well as detection strategies to probe them. Here, we show that current and near-future atomic physics experiments can probe physical models of relaxion dark matter in scenarios of bound relaxion halos around the Earth or Sun.

[1] Department of Particle Physics and Astrophysics, Weizmann Institute of Science, 761001 Rehovot, Israel. [2] Helmholtz Institute Mainz, Johannes Gutenberg University, Mainz 55099, Germany. [3] Department of Physics, University of California at Berkeley, Berkeley, CA 94720-7300, USA. *email: joshaeby@gmail.com

Resolving the nature of the dark matter (DM) is one of the most fundamental questions in modern physics[1]. Although particle DM at the electroweak scale is a highly motivated solution[2], no discovery of such DM was made to date, directly[3–5], indirectly[6], or at the Large Hadron Collider[7]. Another intriguing possibility is that of a cold, ultralight, DM field, coherently oscillating to account for the observed DM density. We consider a class of models where a light scalar particle composes the DM. A well-motivated example is the relaxion, where even a minimal model that addresses the hierarchy problem[8] may lead to the right relic abundance in a manner similar to axion models, however geared with a dynamical misalignment mechanism[9] for relaxion masses roughly above $m_\phi \gtrsim 10^{-11}$ eV. Due to spontaneous Charge-Parity (CP) violation, the relaxion mixes with the Higgs, and, as a result, acquires both pseudoscalar and scalar couplings to the Standard Model (SM) fields[10,11] (this effect could be suppressed in particle-production-based models[12]). The latter distinguishes the relaxion from axion DM, which has only pseudoscalar couplings, and where the same property of generation of CP violation was shown to lead to a solution of the strong CP problem[13] as well as potentially generating the cosmological baryon asymmetry[14].

A striking consequence of the relaxion-Higgs mixing is that, as the relaxion forms a classical oscillating DM background, all basic constants of nature effectively vary with time since they all depend on the Higgs vacuum expectation value[9]. For earlier discussion in the context of dilaton DM, see refs. [15–17]. There are active experimental efforts searching for this form of scalar DM (e.g. refs. [18–24]). Despite the unprecedented accuracy achieved by the various searches, none of the current experiments reach the sensitivity required to probe physically motivated models. Furthermore, the resulting sensitivity in the region of our main interest, characterized by oscillation frequencies above the Hz level, is weaker than that of the probes related to fifth-force searches and equivalence-principle tests (see e.g. refs. [10,15–17,20,21,24–27]).

In this paper, we demonstrate that if the scalar DM forms a self-gravitating compact object, usually known as a "boson star", its density would be higher than that of the local DM density, resulting in enhanced signals for table-top detectors, among others. Furthermore, we raise the possibility that these objects may be trapped by the gravitational potential of the Earth or the Sun. This leads to formation of a "relaxion halo" with a much larger density, compared to that of local DM. We discuss several implications and also detection strategies that are presented below. We work in natural units, where $\hbar = c = 1$.

Our results show that if light scalars like relaxions exist in self-gravitating configurations, they can be probed through transient encounters with the Earth only in the mass range of roughly $m_\phi \gtrsim 4 \times 10^{-8}$ eV; at smaller relaxion masses, either the encounter rate is much lower than $1\,\mathrm{yr}^{-1}$, or the density of the self-gravitating object is lower than the background DM density. In such cases, current experiments are unlikely to gain from the encounter of a relaxion object. However, over a wide range of masses $10^{-16}\,\mathrm{eV} \lesssim m_\phi \lesssim 10^{-8}\,\mathrm{eV}$, we also show that if a large density of relaxion field becomes bound to the Earth or Sun, existing experiments can see great improvements in sensitivity and potentially probe an extended parameter space of physical models.

Results

Coherent DM background. For concreteness, among all possible relaxion couplings to SM particles, we focus on the following interactions:

$$\mathcal{L} \supset g_e \phi\, \bar{e}\, e + \frac{g_\gamma}{4} \phi\, F_{\mu\nu} F^{\mu\nu}, \tag{1}$$

where ϕ is the scalar DM field, e is the electron field, and $F^{\mu\nu}$ is the electromagnetic field strength. The oscillation of the scalar field induces an oscillation in the electron mass, m_e, and the fine structure constant, α, with frequency $\omega \approx m_\phi$. For this reason, atomic precision measurements looking for variation of fundamental constants can probe models of scalar-field DM. For the following discussion, we take a phenomenological approach and consider g_e and g_γ as independent parameters (see refs. [28,29] for possible microscopic origins of these couplings).

A concrete instantiation of this scenario is the relaxion, which has a potential of the form[8–10]

$$V(H,\phi) = \left(\Lambda^2 - g\,\Lambda\,\phi\right)|H|^2 - c\,g\,\Lambda^3\,\phi - \frac{\Lambda_{\rm br}^4}{v^2}|H|^2\,\cos\frac{\phi}{f}, \tag{2}$$

where Λ is the cutoff scale for the Higgs mass, $g \sim \Lambda_{\rm br}^4/f\,\Lambda^3$ is a dimensionless coupling parameter, c is an $\mathcal{O}(1)$ coefficient, $\Lambda_{\rm br}$ is the backreaction scale, and v is the electroweak scale. In this proposal, the rolling of the field ϕ due to the linear term dynamically scans the Higgs mass parameter, until eventually the backreaction potential stops the rolling when $\langle H\rangle = \mathcal{O}(v)$, solving the electroweak hierarchy problem[8]. It was shown recently that with minimal additional assumption about the inflation sector, such a relaxion naturally makes a viable DM candidate[9]. The DM energy density is generated by the misalignment mechanism after the rolling stops, from coherent oscillations of the field around its minimum generated during reheating. The model dependence can be simplified by parameterizing the theory in terms of $T_{\rm ra}$, the temperature at which the backreaction potential reappears after reheating.

For the relaxion model (or other Higgs portal-like theories), scalar couplings to matter are generated by mixing with the Higgs[10,11], and so can be parameterized by a mixing angle $\sin\theta$; for the couplings of Eq. (1), one has $g_e = y_e \sin\theta$ and $g_\gamma \sim (\alpha/4\pi v)\sin\theta$, where y_e is the Higgs Yukawa coupling to the electron. By generic naturalness arguments, one may additionally require $g_e \lesssim 4\pi m_\phi/\Lambda$. We will use this model as a benchmark for comparison, though our conclusions will hold more generally for many forms of light scalar DM.

To investigate whether the variation of fundamental constants induced by the ϕ-oscillation is measurable, we must compute variations of fundamental constants in terms of the model parameters,

$$\frac{\delta m_e}{\langle m_e\rangle} = \frac{g_e\phi}{\langle m_e\rangle}, \qquad \frac{\delta\alpha}{\alpha} = g_\gamma\phi, \tag{3}$$

where $\langle m_e\rangle$ corresponds to the time-averaged electron mass (see Discussion in refs. [21,30]). Given the experimental sensitivity to $\delta m_e/\langle m_e\rangle$ and $\delta\alpha/\alpha$, and also the amplitude of the ϕ-oscillation in a given model, we can estimate the sensitivity to g_e and g_γ.

For a light scalar field with $m_\phi \gtrsim 10^{-10}$ eV, there has been in a blind spot for experimental measurements of time variations of fundamental constants (see ref. [17] for a recent review). In ref. [21], using dynamical decoupling with trapped ions resulted in a bound on scalar particle masses in the range $m_\phi \sim 10^{-11} - 10^{-10}$ eV (roughly 1–10 kHz oscillation frequency) with an accuracy of $1 : 10^{13-14}$ for both $\delta m_e/\langle m_e\rangle$ and $\delta\alpha/\alpha$. The bound was obtained via atom-cavity comparison[31], where for $\delta m_e/\langle m_e\rangle$, this method can only be effectively used for frequencies $\gtrsim$10 kHz[20]. These bounds can be improved by roughly two

orders of magnitude and can cover the range up to 10 MHz. A broader range of masses corresponding to frequencies up to 100 MHz can be covered using conventional Doppler-free techniques such as polarization spectroscopy, using optical transitions in atoms and molecules contained in vapor cells. Assuming 1 year total of interrogation time can effectively bring the sensitivity to roughly $1{:}10^{18}$ (ref. [32]).

At smaller masses $m_\phi \lesssim 10^{-13}$ eV, the best bounds on $\delta m_e/\langle m_e\rangle$ arise from atomic-clock comparisons between hyperfine and optical transitions, which have a relative projected accuracy of roughly $1:10^{16}$ where the hyperfine clock uncertainty is saturated (see, for example, ref. [33]). As for $\delta\alpha/\alpha$, different atomic-clock comparisons[34] as well as measurements of special "forbidden" transitions in highly charged ions to optical transitions can reach accuracies of roughly $1{:}10^{18-19}$ (refs. [35,36]).

If this scalar coherent oscillation corresponds to DM in our local neighborhood, the amplitude is fixed. It is given, within a coherent patch, as (see e.g. refs. [15,25])

$$\phi(t) = \frac{\sqrt{2\rho_{\rm local}}}{m_\phi}\sin(m_\phi t) = 3\times 10^{-3}\ \text{eV}\times\left(\frac{1\ \text{eV}}{m_\phi}\right)\sin(m_\phi t), \tag{4}$$

where we take $\rho_{\rm local} = 0.4\ \text{GeV/cm}^3$ as the local DM density. Various theoretical and experimental efforts have been put forward to probe effective variation of fundamental constants induced by a coherently oscillating background DM field. As it can be seen from Eq. (4), the effect is strongest when the mass is the lightest, $m_\phi \simeq 10^{-21}$ eV, which is marginally allowed by the observation of large-scale structures of the universe[37,38] or measured rotational velocities in galaxies[39]. Substituting this expression to Eq. (3), one can compute the variation of fundamental constants, but the resulting effect is small; in the range $m_\phi \gtrsim 10^{-15}$ eV, the sensitivity estimates discussed above suggest it is difficult to compete with the bounds that arise from fifth-force experiments[18,19,24]. At smaller masses $10^{-21}\ \text{eV} \le m_\phi \le 10^{-15}$ eV, atomic-clock comparison tests (see e.g. ref. [17] and references therein) can compete with or be stronger than fifth-force constraints, though this range does not overlap with the region of relaxion DM models[9].

Relaxion stars. In this section, we consider the case where the scalar DM forms a bound state with much larger density compared to background DM, due to its own self-gravity and self-interactions. These are typically known as boson stars or axion stars (or in the more specific case, relaxion stars). Here, we investigate whether atomic precision measurements can probe the existence of such compact objects when they pass through the Earth. A boson star is described by a classical scalar field, oscillating coherently with frequency approximately equal to the scalar particle mass. Similar to the discussion above, a crucial quantity for precision measurement is the amplitude of oscillation, $\phi = \sqrt{2\rho_\star}/m_\phi$, which is determined by the density $\rho_\star$ of the compact object. Note that we have dropped the explicit time dependence of ϕ for notational simplicity, and will from now on take ϕ as the amplitude and m_ϕ as the frequency of oscillation.

Formation of boson stars is a rapidly evolving field. In the context of QCD axions, overdensities known as miniclusters can be produced on small physical scales (compared to the scale of galaxies) if the Peccei-Quinn symmetry is broken after inflation[40]. These miniclusters have been recently shown to form self-gravitating boson stars on short timescales (compared to galaxy lifetimes), through a process described by gravitational relaxation of effective quasiparticles[41,42]; this has been investigated assuming both idealized initial conditions[43], as well as more realistic ones[44] determined by large-scale simulations of QCD axions[45]. For ultralight axions, large-scale simulations also show boson star-like objects forming in the central cores of galaxies[46,47], suggesting that this is a generic property of light scalar-field DM. The spectrum of initial density fluctuations has not similarly been investigated for relaxions, a topic we delay for future work; for the present purposes, we merely point out that a similar formation mechanism might hold for boson stars formed from relaxions as well.

A compact object is independent of background DM and its density does not necessarily coincide with that of the background. In the presence of gravity, a free scalar field can support itself against collapse through repulsive gradient energy (that is, effective pressure sourced by the kinetic energy of the field); this leads to a unique relation between its radius $R_\star$ and mass $M_\star$,

$$R_\star = \frac{M_{\rm Pl}^2}{m_\phi^2}\frac{2}{M_\star}, \tag{5}$$

where $M_{\rm Pl} = 1.2\times 10^{19}$ GeV is the Planck mass. Some generic properties of boson stars are reviewed in Supplementary Note 1. The overdensity inside a boson star compared to the background density of DM would correspond to

$$\delta \equiv \frac{\rho_\star}{\rho_{\rm local}} = \frac{2\ M_{\rm Pl}^2}{7\pi\ m_\phi^2\ R_\star^4}\frac{1}{\rho_{\rm local}} \approx 7\times 10^{21}\left(\frac{10^{-10}\text{eV}}{m_\phi}\right)^2\left(\frac{10^5\,\text{km}}{R_\star}\right)^4, \tag{6}$$

where we used the approximate profile of Supplementary Eq. (S.5) at $r \ll R_\star$. In this estimation, the benchmark choice for m_ϕ is consistent with the concrete relaxion DM model described in ref. [9]; in this case, we would expect to gain a $\sqrt{\delta}\approx 10^{11}$ enhancement in the amplitude of ϕ if such an object passes through the Earth. This leads to a relatively large effective variation of fundamental constants, compared to the case where such variation is induced by the standard background DM density.

However, the encounter rate between such stars and the Earth is low. To estimate how many such encounters would take place per year, we assume that an $\mathcal{O}(1)$ fraction of local DM is in the form of stable bound states with a fixed mass $M_\star$; the actual distribution of boson star masses depends critically on the formation history, which is beyond the scope of this paper. We also assume a geometric cross-section $\sigma_\star = \pi\ R_\star^2$, and that the motion of the boson stars obeys the virial relation in terms of their typical distribution, implying a speed of $v_\star = 10^{-3}$. Under these assumptions, the encounter rate between the Earth and such objects is

$$\Gamma = n_\star\sigma_\star v_\star = \frac{\rho_{\rm local}}{M_\star}\pi\ R_\star^2\ v_\star \approx 2\times 10^{-18}\,\text{yr}^{-1}\left(\frac{m_\phi}{10^{-10}\text{eV}}\right)^2\left(\frac{R_\star}{10^5\,\text{km}}\right)^3. \tag{7}$$

From this estimate, we see that these encounters are so rare that an encounter typically does not occur during the entire history of the universe. More generally, the encounter rate increases with smaller δ as

$$\Gamma \approx 0.05\,\text{yr}^{-1}\times\delta^{-3/4}\sqrt{\frac{m_\phi}{10^{-10}\,\text{eV}}}. \tag{8}$$

In Fig. 1a, we identify the parameter space of relaxion mass m_ϕ and decay constant f in which a collision rate $\Gamma = 1\ \text{yr}^{-1}$ is possible. Although we ignore the self-interactions of relaxions, we include the decay constant f in the plot to present a benchmark relaxion DM model (black solid lines allowed parameters, dashed

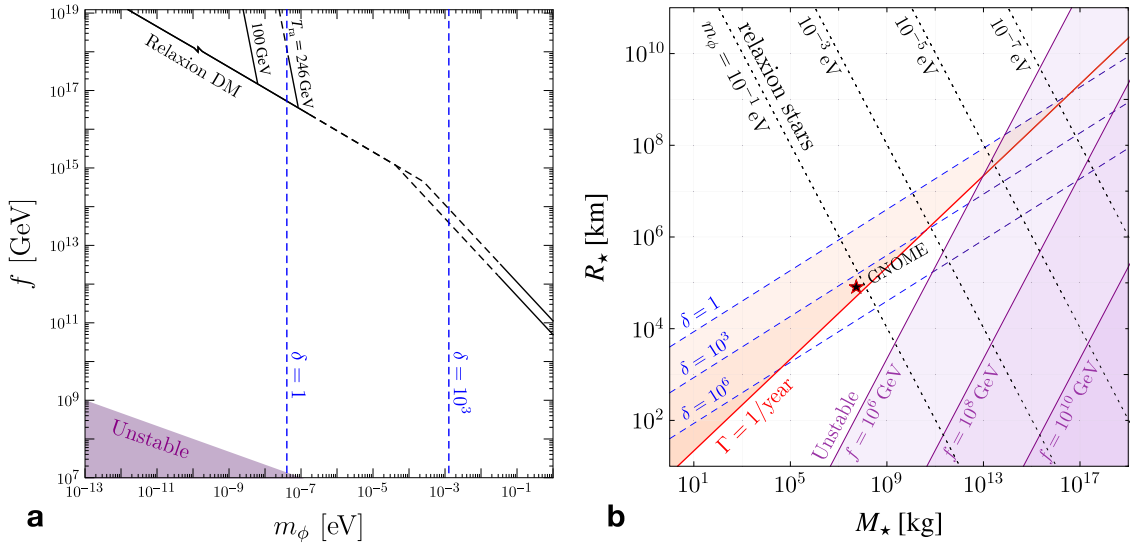

Fig. 1 The relevant parameter space for transient dark matter (DM) boson stars encountering the Earth. **a** Parameter space in scalar mass m_ϕ and decay constant f allowing for gravitationally stable objects, assuming the encounter rate is $\Gamma = 1\,\mathrm{yr}^{-1}$. The dashed blue lines are contours of constant overdensity δ, and the purple shaded regions indicate instability through self-interactions. The black lines denote coherent relaxion DM for different choices of T_{ra}, the temperature at which the relaxion backreaction potential reappears after reheating; solid lines are allowed parameters, and dashed are ruled out by fifth-force constraints (see ref. [9] for further information). **b** $M_\star$ and $R_\star$ are treated as independent parameters; the black dotted lines denote stable configurations formed from scalars of mass m_ϕ, and the red shaded region represents $\Gamma > 1\,\mathrm{yr}^{-1}$ and $\delta > 1$. The blue lines and purple shaded regions are the same as in **a**. The black star represents the benchmark point used by the GNOME collaboration[48].

ruled out by fifth-force meaurements)[9] and the region where the relaxion star is unstable due to the self-interaction (purple shaded region, see Supplementary Eq. (S.11) for details regarding the self-interaction potential). The overdensity δ is also denoted by blue dashed lines, assuming the rate of one collision per year. If $m_\phi \lesssim 10^{-8}$ eV, an overdensity $\delta > 1$ along with $\Gamma = 1\,\mathrm{yr}^{-1}$ is not possible for a self-gravitating object; only if $m_\phi > 10^{-8}$ eV is this scenario viable. This mass range corresponds to frequencies greater than order MHz, which can be probed using experimental techniques discussed in the Coherent DM Background.

Note that for the case of axion-like particles (ALPs), it has been proposed that pseudoscalar coupling to nucleons can be probed by using nuclear magnetic resonance techniques even when $m_\phi \gtrsim 10^{-8}$ eV and $\delta = 1$ (ref. [49]). Although we do not discuss it in this paper, this experimental technique can equally apply to the scenario of transient relaxion stars since the relaxion could also have pseudoscalar coupling to the SM fields.

In Fig. 1b, we show the mass-radius relation of boson stars (dotted lines). Similar to the Fig. 1a, the purple shaded region denotes boson stars that are unstable to collapse due to self-interactions, while the blue dashed lines denote the density contrast $\delta = \rho_\star/\rho_{\mathrm{local}}$. The red shaded region represents $\delta > 1$ and $\Gamma > 1\,\mathrm{yr}^{-1}$, which is attainable only for $m_\phi \gtrsim 10^{-8}$ eV. In other words, for scalar mass $m_\phi \lesssim 10^{-8}$ eV, it is either the case that the density of boson star is large but its encounter rate is too small for terresterial experiments, or that the rate is large enough but its density becomes even smaller than that of the background DM. Note that possible transient signals induced by axion stars have already been investigated in ref. [48], where it is concluded that the Global Network of Optical Magnetometers for Exotic physics searches (GNOME) can probe parameter space of ALPs for $m_{\mathrm{ALP}} < 10^{-13}$ eV, and that the projected sensitivity surpasses astrophysical constraints, which may seem to contradict Fig. 1. In ref. [48], the approach taken is more phenomenological, assuming $M_\star$ and $R_\star$ to be fully independent, which allows some region of parameter space to be probed by simultaneously satisfying $\Gamma = \mathcal{O}(1)\,\mathrm{yr}^{-1}$ and $\delta \gg 1$. This also indicates that the axion stars considered in ref. [48] are not truly ground-state configurations. We show the benchmark point used in ref. [48] ($R_\star = 10R_\oplus$ and $M_\star = 4\times 10^7$ kg) as the black star in the figure.

Relaxion halo. The formation of boson stars is a complex dynamical process. Typical investigations involve simulations of scalar-field dynamics, and commonly neglect any effect from baryons[40,43,45]. In this section we suggest that, in the presence of baryons, gravitational relaxation may lead to configurations in which a large density of scalar field becomes bound to an external gravitational source. The resulting compact object in this case could be sustained by the gravitational field of an external massive body instead of its own self-gravity. We will refer to an object of this kind as a relaxion halo. There are significant uncertainties associated with this scenario, which we will return to in future work. Here, we assume such a halo can exist and investigate the consequences in terrestrial experiments.

We focus on the relaxion halo hosted by the Sun and by the Earth. In this case, M_{ext} is either the mass of the Sun or the Earth, and R_{ext} is the corresponding radius. Assuming $M_\star \ll M_{\mathrm{ext}}$, the radius of a relaxion halo is

$$R_\star \equiv \begin{cases} \frac{M_{\mathrm{Pl}}^2}{m_\phi^2}\frac{1}{M_{\mathrm{ext}}} & \text{for } R_\star > R_{\mathrm{ext}}\ , \\ \left(\frac{M_{\mathrm{Pl}}^2}{m_\phi^2}\frac{R_{\mathrm{ext}}^3}{M_{\mathrm{ext}}}\right)^{1/4} & \text{for } R_\star \le R_{\mathrm{ext}}\ . \end{cases} \quad (9)$$

The radius of a relaxion halo is determined by the gravitational potential of the external source. In the first case, $R_\star > R_{\mathrm{ext}}$, we approximate the external source as a point-like mass, which results in an exponential relaxion-halo profile, Supplementary Eq. (S.8) In the second case, $R_\star < R_{\mathrm{ext}}$, we approximate the external source as a constant-density sphere, where the gravitational potential is given as that of a harmonic oscillator and the profile is Gaussian, Supplementary Eq. (S.9); though this approximation is rough in principle, in practice it works well when $R_\star \gg R_{\mathrm{ext}}$, and

to go beyond it is outside the scope of this work. See Supplementary Note 1 for details regarding these two profiles. Note that in both of these cases, the radius is independent of $M_\star$. We only consider $M_\star < M_{\rm ext}/2$ for $R_\star > R_{\rm ext}$, and $M_\star < (M_{\rm ext}/2)(R_\star/R_{\rm ext})^3$ for $R_\star < R_{\rm ext}$, ensuring that the self-gravity is subdominant.

In the presence of an external gravitational source of mass $M_{\rm ext}$, the ground-state profile for a relaxion halo is modified compared to the relaxion star. To obtain the density and the amplitude of oscillation, we use exponential and Gaussian profiles for $R_\star > R_{\rm ext}$ and $R_\star \leq R_{\rm ext}$, respectively (Supplementary Eqs. (S.8 and S.9)) The asymptotic behavior of the halo density is

$$\rho_\star \propto \begin{cases} \exp(-2r/R_\star) & \text{for } R_\star > R_{\rm ext}\ , \\ \exp\left(-r^2/R_\star^2\right) & \text{for } R_\star \leq R_{\rm ext}\ . \end{cases} \tag{10}$$

The relevant quantity for experimental searches is the density of relaxion field at the surface of the Earth. We see from Eq. (3) that the variation of fundamental constants is given by $\delta m_e/\langle m_e\rangle = g_e\sqrt{2\rho_\star}/(\langle m_e\rangle m_\phi)$ and $\delta\alpha/\alpha = g_\gamma\sqrt{2\rho_\star}/m_\phi$. We discuss various probes to detect these effects in the next section.

One can determine an upper bound on the mass $M_\star$ of a relaxion halo through gravitational observations. In the case of an Earth-based halo, the strongest constraint arises from lunar laser ranging[50], and for a Solar-based halo, from planetary ephemerides[51]; both are described in the Supplementary Note 2. Note that we consider other possible constraints on an Earth halo in Supplementary Note 3, but conclude that ref. [50] represents the strongest constraint. We show the derived constraint on the mass of a relaxion halo as a function of the scalar particle mass m_ϕ in Fig. 2. Using the result of $(M_\star)_{\rm max}$, we obtain the scalar-field value ϕ, which is directly related to the observables, $\delta m_e/\langle m_e\rangle$ and $\delta\alpha/\alpha$, which we discuss in the next section.

Finally, we comment on the coherence properties of the relaxion halo oscillations. Because a relaxion halo is supported against collapse by gradient energy, the coherence length of the halo is nothing other than its radius; that is,

$$R_{\rm coh} = \frac{1}{m_\phi\, v} = \frac{1}{m_\phi}\sqrt{\frac{R_\star\, M_{\rm Pl^2}}{M_{\rm ext}}} = R_\star, \tag{11}$$

where v is the velocity dispersion in the halo. The coherence time can be estimated similarly; for a relaxion Earth halo, we find

$$\tau_{\rm coh} = \frac{1}{m_\phi\, v^2} = m_\phi\, R_\star^2 \approx \begin{cases} 10^3\ {\rm s}\ \left(10^{-9}{\rm eV/m_\phi}\right)^3 & \text{for } R_\star > R_\oplus\ , \\ 10^3\ {\rm s} & \text{for } R_\star \leq R_\oplus\ , \end{cases} \tag{12}$$

where we used the radii of Eq. (9) with $M_{\rm ext} = M_\oplus$. For a Solar halo, the coherence time is at least two orders of magnitude larger, as it is enhanced by a large $R_\star \gtrsim 1$ AU in that case.

Hunting for relaxion halos with table-top experiments. As explained above, the possibility of relaxion halos surrounding the Earth or the Sun may lead to an enhanced signal in various table-top experiments. Using the maximally allowed relaxion halo mass as an input, and also using the approximate form of scalar-field profile described in Supplementary Note 1, we can compute the oscillation amplitude and compare it to the corresponding experimental sensitivities. In order to study the present/near-future sensitivity, we consider the following four cases: (i) solar-based relaxion halo which is relevant for $m_\phi \sim 10^{-15}$ eV—bounds on $\delta m_e/\langle m_e\rangle$ and on $\delta\alpha/\alpha$ are separately considered; (ii) Earth-based relaxion halo which is relevant for $m_\phi \sim 10^{-10}$ eV—bounds on $\delta m_e/\langle m_e\rangle$ and on $\delta\alpha/\alpha$ are separately considered.

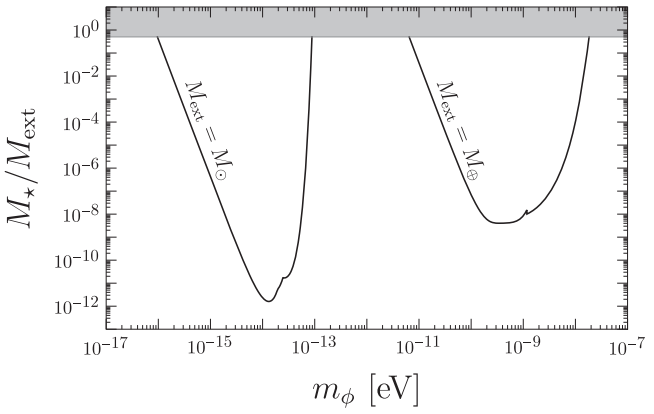

Fig. 2 The upper bound $(M_\star)_{\rm max}$ on the relaxion halo mass $M_\star$ as a function of scalar particle mass m_ϕ; the regions above the black lines are excluded by either (right side, assuming an Earth halo) lunar laser ranging[50], or (left side, assuming a Solar halo) planetary ephemerides[51]. We also require $M_\star \leq M_{\rm ext}/2$ (boundary of gray shaded region), such that our assumption $M_\star \ll M_{\rm ext}$ is satisfied throughout.

For case (i), we show in Fig. 3 sensitivity curves for $(\delta m_e/\langle m_e\rangle,\ \delta\alpha/\alpha) = 10^{-16}$ (solid lines) and 10^{-18} (dashed lines). In addition, the bounds from fifth-force and equivalence-principle tests correspond to the shaded region[52–55], the red line corresponds to the naturalness limit with a cutoff at $\Lambda = 3$ TeV (the minimal allowed cutoff consistent with solving the hierarchy problem), and the green line corresponds to the naive upper limit on coupling constants which derived from scalar-Higgs portal models[56]. Note that the bounds from equivalence-principle tests are obtained by neglecting the other possible couplings of scalar field to SM particles.

In Fig. 4, we show the analogous sensitivities in case (ii), with $(\delta m_e/\langle m_e\rangle,\ \delta\alpha/\alpha) = 10^{-14}$ (solid), 10^{-16} (dashed), and 10^{-18} (dotted). In the case of a Solar halo, future projections for g_e reach the parameter space where the scalar mass is technically natural, while in the case of an Earth halo, future projections reach not only to the naturalness limit for g_e and g_γ, but also to the region of physically motivated generic relaxion models[10,26]. The shaded regions represent the allowed parameter space for coherent relaxion DM[9], taking $g_e = y_e\ \sin\theta$ and $g_\gamma = (\alpha/4\pi v)\ \sin\theta$; in Fig. 4, the brown region is for $y_e = y_e^{\rm SM}$ (the SM prediction), whereas the blue region is for $y_e = 600\times y_e^{\rm SM}$, the maximum allowed value given current LHC constraints[57].

Discussion

In this work, we consider the effect of (pseudo)scalar-field DM, e.g. relaxion DM, in atomic physics experiments. We propose that such DM can form gravitationally bound objects denoted as boson stars (or relaxion stars), and suggest that these stars can be formed around the Earth or the Sun leading to relaxion halos with density well above that of the local DM. Due to the mixing with the Higgs, the oscillating DM background implies that all the fundamental couplings of nature are varying with time. This implies that one could search for signals of such objects in table-top experiments, which may be probed in the near future with projected sensitivity stronger than that of fifth-force and equivalence-principle tests. In this scenario, even present experimental sensitivity[21,32] may be sufficient to probe the parameter space of coherent relaxion DM[9].

We note that as our signal is related to rapid-oscillation signals, other existing probes of scalar DM, which are direct-current

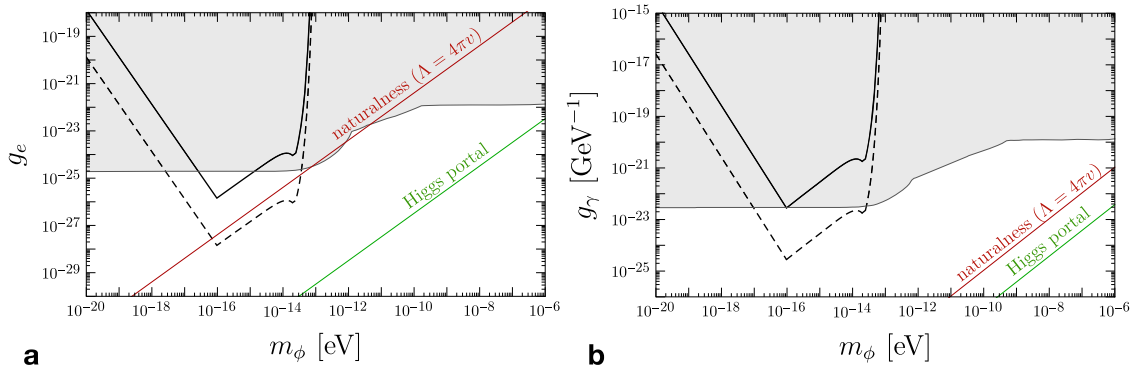

Fig. 3 Projected sensitivity of table-top experiments in the presence of a relaxion Solar halo. **a** Projected constraints on g_e. Experimental sensitivities in $\delta m_e/\langle m_e\rangle$ are taken to be 10^{-16}, 10^{-18} (solid and dashed lines, respectively). The gray shaded region is excluded by fifth-force experiments. The red line is the naturalness limit, where the cutoff is taken to be $\Lambda = 3$ TeV, while the green line is an upper limit on coupling constants which can be obtained from physical relaxion models. The halo mass is taken as $M_\star = \min[(M_\odot/2)(R_\star/R_\odot)^3, (M_\star)_{\rm max}]$, where $(M_\star)_{\rm max}$ is the maximum relaxion halo mass allowed by existing gravitational constraints. **b** Projected constraints on g_γ. Experimental sensitivities in $\delta\alpha/\alpha$ are taken to be 10^{-16} and 10^{-18} (solid and dashed lines, respectively).

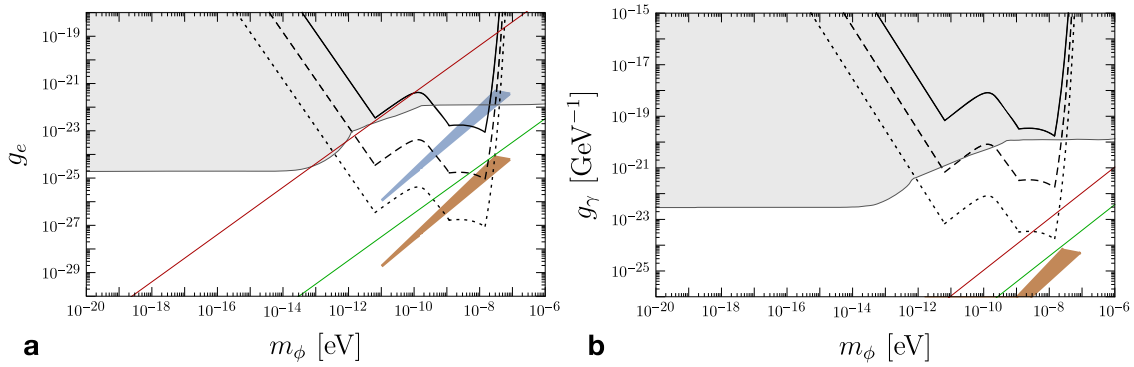

Fig. 4 Projected sensitivity of table-top experiments in the presence of a relaxion Earth halo. **a** Projected constraints on g_e. Experimental sensitivities in $\delta m_e/\langle m_e\rangle$ are taken to be 10^{-14}, 10^{-16}, and 10^{-18} (solid, dashed, and dotted lines, respectively). The gray shaded region is excluded by fifth-force experiments. The red line is the naturalness limit, where the cutoff is taken to be $\Lambda = 3$ TeV, while the green line is an upper limit on coupling constants which can be obtained from physical relaxion models. The halo mass is taken as $M_\star = \min[(M_\oplus/2)(R_\star/R_\oplus)^3, (M_\star)_{\rm max}]$, where $(M_\star)_{\rm max}$ is the maximum relaxion halo mass allowed by existing gravitational constraints. The blue and brown shaded regions represent the allowed regions for coherent relaxion dark matter[9], assuming the electron-Higgs Yukawa coupling is equal to the Standard Model value (blue) or saturates the experimental upper bound (brown). **b** Projected constraints on g_γ. Experimental sensitivities in $\delta\alpha/\alpha$ are taken to be 10^{-14}, 10^{-16}, and 10^{-18} (solid, dashed, and dotted lines, respectively).

oriented and/or using less precise clocks[58–61] would be less sensitive to the above form of DM. However, in the case of a relaxion halo or star which coherently oscillates over sufficiently large distances one may improve the sensitivity to its presence by comparing the phase of the oscillation between two distant experiments (or network of sensors) that are synched to the same external clock, or similarly if a single experiment is to repeat its measurements multiple times while being synchronized to an external clock. Furthermore, there are several proposals for sending high performance clock-systems to space[62,63], which would allow to map the relaxion halo density as a function of distance from the Earth's surface.

Another interesting implication is the possible presence of mini-relaxion halos, whose radius is smaller than that of the Earth so that such halos do not contribute to the signals described above. Such objects arise when the relaxion particle mass is around nano-eV or above. Although they can have densities close to that of the Earth, it is in general difficult to probe them because they are located beneath the surface of the Earth (see however ref. [64], which proposes to test clock universality in deep underground/underwater experiments).

We finally reiterate that our discussion and conclusion throughout the paper holds for any form of light scalar DM, thus covering a large parameter space of well-motivated DM models.

Methods

Further information regarding the methods and techniques used to obtain the results can be found in the Supplementary Material.

Data availability

All data in this paper can be reproduced using the methodology described.

Code availability

The code for analyzing the numerical results and producing the figures was written using Mathematica 10, and the files can be made available upon request.

Received: 3 April 2019; Accepted: 11 November 2019;
Published online: 07 January 2020

References

1. Bertone, G. & Hooper, D. History of dark matter. *Rev. Mod. Phys.* **90**, 045002 (2018).
2. Jungman, G., Kamionkowski, M. & Griest, K. Supersymmetric dark matter. *Phys. Rep.* **267**, 195–373 (1996).
3. Bertone, G., Hooper, D. & Silk, J. Particle dark matter: evidence, candidates and constraints. *Phys. Rep.* **405**, 279–390 (2005).
4. da Silva, C. F. P. Dark matter searches with LUX. In *Proc. 52nd Rencontres de Moriond on Very High Energy Phenomena in the Universe,* La Thuile, Italy, 18–25 March 2017, 199–209 (2017).
5. Aprile, E. et al. Dark matter search results from a one ton-year exposure of XENON1T. *Phys. Rev. Lett.* **121**, 111302 (2018).
6. Gaskins, J. M. A review of indirect searches for particle dark matter. *Contemp. Phys.* **57**, 496–525 (2016).
7. Boveia, A. & Doglioni, C. Dark matter searches at colliders. *Ann. Rev. Nucl. Part. Sci.* **68**, 429–459 (2018).
8. Graham, P. W., Kaplan, D. E. & Rajendran, S. Cosmological relaxation of the electroweak scale. *Phys. Rev. Lett.* **115**, 221801 (2015).
9. Banerjee, A., Kim, H. & Perez, G. Coherent relaxion dark matter. Preprint at http://arXiv.org/1810.01889 [hep-ph] (2018).
10. Flacke, T., Frugiuele, C., Fuchs, E., Gupta, R. S. & Perez, G. Phenomenology of relaxion-Higgs mixing. *J. High Energy Phys.* **06**, 050 (2017).
11. Choi, K. & Im, S. H. Constraints on relaxion windows. *J. High Energy Phys.* **12**, 093 (2016).
12. Hook, A. & Marques-Tavares, G. Relaxation from particle production. *J. High Energy Phys.* **12**, 101 (2016).
13. Davidi, O., Gupta, R. S., Perez, G., Redigolo, D. & Shalit, A. The Nelson-Barr relaxion. *Phys. Rev.* **D99**, 035014 (2019).
14. Abel, S. A., Gupta, R. S. & Scholtz, J. Out-of-the-box baryogenesis during relaxation. *Phys. Rev.* **D100**, 015034 (2019).
15. Arvanitaki, A., Huang, J. & Van Tilburg, K. Searching for dilaton dark matter with atomic clocks. *Phys. Rev.* **D91**, 015015 (2015).
16. Graham, P. W., Kaplan, D. E., Mardon, J., Rajendran, S. & Terrano, W. A. Dark matter direct detection with accelerometers. *Phys. Rev.* **D93**, 075029 (2016).
17. Safronova, M. S. et al. Search for new physics with atoms and molecules. *Rev. Mod. Phys.* **90**, 025008 (2018).
18. Van Tilburg, K., Leefer, N., Bougas, L. & Budker, D. Search for ultralight scalar dark matter with atomic spectroscopy. *Phys. Rev. Lett.* **115**, 011802 (2015).
19. Hees, A., Guena, J., Abgrall, M., Bize, S. & Wolf, P. Searching for an oscillating massive scalar field as a dark matter candidate using atomic hyperfine frequency comparisons. *Phys. Rev. Lett.* **117**, 061301 (2016).
20. Geraci, A. A., Bradley, C., Gao, D., Weinstein, J. & Derevianko, A. Searching for ultra-light dark matter with optical cavities. *Phys. Rev. Lett.* **123**, 031304 (2019).
21. Aharony, S. et al. Constraining rapidly oscillating scalar dark matter using dynamic decoupling. Preprint at http://arXiv.org/1902.02788 [hep-ph] (2019).
22. Stadnik, Y. V. & Flambaum, V. V. Improved limits on interactions of low-mass spin-0 dark matter from atomic clock spectroscopy. *Phys. Rev.* **A94**, 022111 (2016).
23. Stadnik, Y. V. & Flambaum, V. V. Can dark matter induce cosmological evolution of the fundamental constants of Nature? *Phys. Rev. Lett.* **115**, 201301 (2015).
24. Rosenband, T. et al. Frequency ratio of Al and Hg single-ion optical clocks; metrology at the 17th decimal place. *Science* **319**, 1808–1812 (2008).
25. Arvanitaki, A., Dimopoulos, S. & Van Tilburg, K. Sound of dark matter: searching for light scalars with resonant-mass detectors. *Phys. Rev. Lett.* **116**, 031102 (2016).
26. Frugiuele, C., Fuchs, E., Perez, G. & Schlaffer, M. Relaxion and light (pseudo) scalars at the HL-LHC and lepton colliders. *J. High Energy Phys.* **10**, 151 (2018).
27. Hees, A., Minazzoli, O., Savalle, E., Stadnik, Y. V. & Wolf, P. Violation of the equivalence principle from light scalar dark matter. *Phys. Rev.* **D98**, 064051 (2018).
28. Gupta, R. S., Komargodski, Z., Perez, G. & Ubaldi, L. Is the relaxion an axion? *J. High Energy Phys.* **02**, 166 (2016).
29. Davidi, O., Gupta, R. S., Perez, G., Redigolo, D. & Shalit, A. The hierarchion, a relaxion addressing the standard models hierarchies. *J. High Energy Phys.* **08**, 153 (2018).
30. Kozlov, M. G. & Budker, D. Comment on sensitivity coefficients to variation of fundamental constants. *Ann. Phys.* **531**, 1800254 (2018).
31. Wcislo, P. et al. Experimental constraint on dark matter detection with optical atomic clocks. *Nat. Astron.* **1**, 0009 (2016).
32. Antypas, D. et al. Scalar dark matter in the radio-frequency band: atomic-spectroscopy search results. *Phys. Rev. Lett.* **123**, 141102 (2019).
33. Guena, J. et al. Progress in atomic fountains at lne-syrte. *IEEE Trans. Ultrason. Ferroelectr. Freq. Control* **59**, 391–409 (2012).
34. Ludlow, A. D., Boyd, M. M., Ye, J., Peik, E. & Schmidt, P. O. Optical atomic clocks. *Rev. Mod. Phys.* **87**, 637–701 (2015).
35. Dzuba, V. A., Safronova, M. S., Safronova, U. I. & Flambaum, V. V. Actinide ions for testing the spatial α -variation hypothesis. *Phys. Rev. A* **92**, 060502 (2015).
36. Kennedy, C. et al. Constraints on ultralight dark matter by atom-cavity comparisons. To be published.
37. Iršič, V., Viel, M., Haehnelt, M. G., Bolton, J. S. & Becker, G. D. First constraints on fuzzy dark matter from Lyman-α forest data and hydrodynamical simulations. *Phys. Rev. Lett.* **119**, 031302 (2017).
38. Armengaud, E., Palanque-Delabrouille, N., Yèche, C., Marsh, D. J. E. & Baur, J. Constraining the mass of light bosonic dark matter using SDSS Lyman-α forest. *Mon. Not. Roy. Astron. Soc.* **471**, 4606–4614 (2017).
39. Bar, N., Blas, D., Blum, K. & Sibiryakov, S. Galactic rotation curves versus ultralight dark matter: Implications of the soliton-host halo relation. *Phys. Rev.* **D98**, 083027 (2018).
40. Kolb, E. W. & Tkachev, I. I. Axion miniclusters and Bose stars. *Phys. Rev. Lett.* **71**, 3051–3054 (1993).
41. Hui, L., Ostriker, J. P., Tremaine, S. & Witten, E. Ultralight scalars as cosmological dark matter. *Phys. Rev.* **D95**, 043541 (2017).
42. Bar-Or, B., Fouvry, J.-B. & Tremaine, S. Relaxation in a Fuzzy dark matter halo. *Astrophys. J.* **871**, 28 (2019).
43. Levkov, D. G., Panin, A. G. & Tkachev, I. I. Gravitational Bose-Einstein condensation in the kinetic regime. *Phys. Rev. Lett.* **121**, 151301 (2018).
44. Eggemeier, B. & Niemeyer, J. C. Formation and mass growth of axion stars in axion miniclusters. *Phys. Rev.* **D100**, 063528 (2019).
45. Vaquero, A., Redondo, J. & Stadler, J. Early seeds of axion miniclusters. *JCAP* **04**, 012 (2019).
46. Schive, H.-Y., Chiueh, T. & Broadhurst, T. Cosmic structure as the quantum interference of a coherent dark wave. *Nat. Phys.* **10**, 496–499 (2014).
47. Veltmaat, J., Niemeyer, J. C. & Schwabe, B. Formation and structure of ultralight bosonic dark matter halos. *Phys. Rev.* **D98**, 043509 (2018).
48. Jackson Kimball, D. F. et al. Searching for axion stars and Q-balls with a terrestrial magnetometer network. *Phys. Rev.* **D97**, 043002 (2018).
49. Jackson Kimball, D. F. et al. Overview of the Cosmic Axion Spin Precession Experiment (CASPEr). Preprint at http://arXiv.org/1711.08999 [physics.ins-det] (2017).
50. Adler, S. L. Placing direct limits on the mass of earth-bound dark matter. *J. Phys.* **A41**, 412002 (2008).
51. Pitjev, N. P. & Pitjeva, E. V. Constraints on dark matter in the solar system. *Astron. Lett.* **39**, 141–149 (2013) [*Astron. Zh.* **39**,163 (2013)].
52. Touboul, P. et al. MICROSCOPE mission: first results of a space test of the equivalence principle. *Phys. Rev. Lett.* **119**, 231101 (2017).
53. Bergé, J. et al. MICROSCOPE mission: first constraints on the violation of the weak equivalence principle by a light scalar dilaton. *Phys. Rev. Lett.* **120**, 141101 (2018).
54. Schlamminger, S., Choi, K. Y., Wagner, T. A., Gundlach, J. H. & Adelberger, E. G. Test of the equivalence principle using a rotating torsion balance. *Phys. Rev. Lett.* **100**, 041101 (2008).
55. Smith, G. L. et al. Short range tests of the equivalence principle. *Phys. Rev.* **D61**, 022001 (2000).
56. Piazza, F. & Pospelov, M. Sub-eV scalar dark matter through the super-renormalizable Higgs portal. *Phys. Rev.* **D82**, 043533 (2010).
57. Dery, A., Frugiuele, C. & Nir, Y. Large Higgs-electron Yukawa coupling in 2HDM. *J. High Energy Phys.* **04**, 044 (2018).
58. Derevianko, A. & Pospelov, M. Hunting for topological dark matter with atomic clocks. *Nat. Phys.* **10**, 933 (2014).
59. Roberts, B. M. et al. Search for domain wall dark matter with atomic clocks on board global positioning system satellites. *Nat. Commun.* **8**, 1195 (2017).
60. Wolf, P., Alonso, R. & Blas, D. Scattering of light dark matter in atomic clocks. *Phys. Rev.* **D99**, 095019 (2019).
61. Derevianko, A. Detecting dark-matter waves with a network of precision-measurement tools. *Phys. Rev.* **A97**, 042506 (2018).
62. Schiller, S. et al. The Space Optical Clocks Project: development of high-performance transportable and breadboard optical clocks and advanced subsystems. ArXiv: Preprint at http://arXiv.org/1206.3765 [quant-ph] (2012).
63. Kolkowitz, S. et al. Gravitational wave detection with optical lattice atomic clocks. *Phys. Rev.* **D94**, 124043 (2016).
64. Flambaum, V. V. & Pospelov, M. Neutrino velocity and the variability of fundamental constants. *Phys. Rev. D* **86**, 107502 (2012).

Acknowledgements

We are grateful for useful discussions and comments on the manuscript from Kfir Blum, Itay Halevy, Eric Kuflik, Mordehai Milgrom, Roee Ozeri, Gil Paz, Stephan Schiller, L.C.R. Wijewardhana, and Hong Zhang. The work of D.B. is supported by the European

Research Council (ERC) under the European Unions Horizon 2020 research and innovation programme (grant agreement No 695405), the Simons and Heising-Simons Foundations and the DFG Reinhart Koselleck project. The work of J.E. is supported by the Zuckerman STEM Leadership Program. The work of G.P. is supported by grants from the BSF, ERC, ISF, Minerva, and the Segre Research Award.

Author contributions

All authors contributed to the scientific discussions and theoretical developments of this work; the original idea of the relaxion halo emerged as a result of these group discussions. The text was co-written also by all authors. D.B. provided background regarding experimental sensitivities and methods in atomic physics. J.E. analyzed boson star configurations and their stability. H.K. derived the gravitational constraints on relaxion halos bound to the Earth and Sun. A.B., H.K., and G.P. provided details regarding the specific relaxion dark matter model analyzed. A.B. and G.P. provided independent checks of all results, and G.P. also supervised the project.

Competing interests

The authors declare no competing interests.

Additional information

Supplementary information is available for this paper at https://doi.org/10.1038/s42005-019-0260-3.

Correspondence and requests for materials should be addressed to J.E.